Journal of Sound and Vibration (1999) **225**(4), 597–610
Article No. jsvi.1998.2109, available online at http://www.idealibrary.com on IDEAL®

VIBRATION CHARACTERISTICS OF SYSTEMS WITH MULTIPLE BLADES

G. X. Ren and Z. C. Zheng
Department of Engineering Mechanics, Tsinghua University, 100084 *Beijing, China*
AND
W. J. Wang
*School of Engineering, University of Sussex, Brighton BN*1 9*QT, England*

(*Received* 20 *November* 1996, *and in final form* 7 *December* 1998)

An interesting phenomenon can be observed when the state-space dynamic substructural method is applied to the eigenproblem of bladed disk–shaft systems: whether or not the shaft is flexible, each frequency of the single root-fixed blade appears as a frequency of the whole structure with a multiplicity of at least $(n-3)$, where n is the number of repetitive blades. The presented result can be regarded as an extension of previous findings by the authors in the sense that the commonly interfaced repetitive substructures are allowed to be treated as a rigid body in modal analysis. The defectiveness issue of the multiple eigenvalues arising from the repetitive substructures is also addressed. Examples of rotary wing models and a simplified turbine model are presented for validation together with attempting their physical explanations.

1. INTRODUCTION

A structure containing repetitive components is very common in engineering, which often brings about multiple eigenvalues in its dynamic analysis. However, in a practical modal test or dynamic numerical computations, real multiple eigenvalues of such structures usually only appear as very closely distributed eigenvalues due to the approximation arising from representing the symmetry in a finite floating point, the uncertainty in applied computing methods or limited precision in manufacturing the product. In most cases, it is hard to tell whether those closely distributed eigenvalues are indeed different close eigenvalues or identical multiple eigenvalues distorted by the approximation or manufacturing precision. The properties of invariant subspaces associated with multiple eigenvalues make it even more difficult to extract those eigenvalues [1, 2]. Furthermore, if multiple eigenvalues are defective, further difficulty in numerically ascertaining the Jordan structure will arise [3]. It is believed that investigating the mechanism of multiple eigenvalues and developing effective numerical methods for extracting those multiple eigenvalues are essential for

0022–460X/99/340597 + 14 $30.00/0

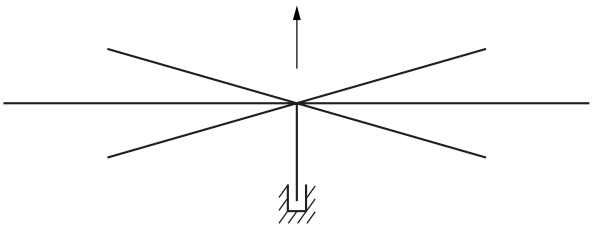

Figure 1. A rotary wing model.

understanding the dynamic characteristics in those types of widely used structures with repetitive substructures.

The dynamic substructure method or the component mode synthesis is an efficient approach to extracting modals from large scale complicated structures [4–8], which is especially convenient for the assembled structures in which the parts are much simpler and easier to be analysed. For those with repetitive substructures, even more advantage should be taken of the geometrical features. In previous research [9, 10], it was found that there should be a class of $(n-3)$ multiple eigenvalues for the rotary wing model, where n is the number of blades. A class of more general structures with $(n-\alpha)$ multiple eigenvalues arising from its repetitive substructures has also been obtained in a more recent investigation [11], in which the n repetitive substructures have a common interface and they are mounted on the rest of the structure only through that common interface, as in the examples illustrated in Figures 1–3. As suggested in reference [11], the so-called block retaining property in applying the dynamic substructure method or the component mode synthesis is advantageous and deserves further investigation. In this paper, research will be extended to more general multi-bladed structural systems, such as in the helicopter rotary wing model and the turbine model shown in Figures 4 and 5, in which the sole common interface of the repetitive substructures will be regarded as a rigid body instead of a flexible one described by a set of degrees-of-freedom. Again the dynamic substructure method is applied to the investigation of the characteristics of multiple eigenvalues arising from the geometric symmetry or repetition, making possible the qualitative modelling of the properties for the whole structure.

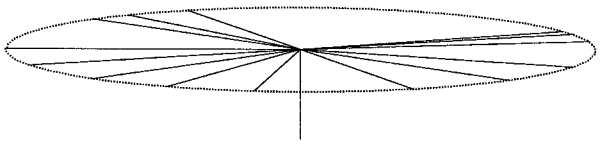

Figure 2. A rotary wing model with non-isotropically distributed blades.

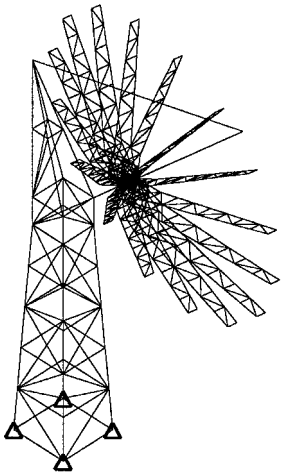

Figure 3. An antenna model.

2. PARTITION AND ANALYSIS OF SUBSTRUCTURES

In the dynamic substructure method, the first step is to partition properly the whole structural system into components according to its geometric and structural identities. In the bladed disk–shaft system, assuming that there are n repetitive blade substructures, counted from the first to the nth substructure, the hub rigid disk then is counted as the $(n + 2)$th substructure and the rest of the structure or shaft as the $(n + 1)$th substructure, the equation of motion for the rth substructure can be written as

$$\mathbf{M}^r\ddot{\mathbf{x}}^r + (\mathbf{G}^r + \mathbf{C}^r)\dot{\mathbf{x}}^r + \mathbf{K}^r\mathbf{x}^r = \mathbf{f}^r + \bar{\mathbf{f}}^r. \quad (r = 1, \cdots, n + 1). \tag{1a}$$

By partitioning equation (1a) according to internal and interface co-ordinates, one has

$$\begin{bmatrix} \mathbf{M}^r_{ii} & \mathbf{M}^r_{ij} \\ \mathbf{M}^r_{ji} & \mathbf{M}^r_{jj} \end{bmatrix} \begin{Bmatrix} \ddot{\mathbf{x}}^r_i \\ \ddot{\mathbf{x}}^r_j \end{Bmatrix} + \left(\begin{bmatrix} \mathbf{G}^r_{ii} & \mathbf{G}^r_{ij} \\ \mathbf{G}^r_{ji} & \mathbf{G}^r_{jj} \end{bmatrix} + \begin{bmatrix} \mathbf{C}^r_{ii} & \mathbf{C}^r_{ij} \\ \mathbf{C}^r_{ji} & \mathbf{C}^r_{jj} \end{bmatrix} \right) \begin{Bmatrix} \dot{\mathbf{x}}^r_i \\ \dot{\mathbf{x}}^r_j \end{Bmatrix}$$
$$+ \begin{bmatrix} \mathbf{K}^r_{ii} & \mathbf{K}^r_{ij} \\ \mathbf{K}^r_{ji} & \mathbf{K}^r_{jj} \end{bmatrix} \begin{Bmatrix} \mathbf{x}^r_i \\ \mathbf{x}^r_j \end{Bmatrix} = \begin{Bmatrix} \mathbf{f}^r_i \\ \mathbf{f}^r_j \end{Bmatrix} + \begin{Bmatrix} \mathbf{0} \\ \bar{\mathbf{f}}^r_j \end{Bmatrix}. \tag{1b}$$

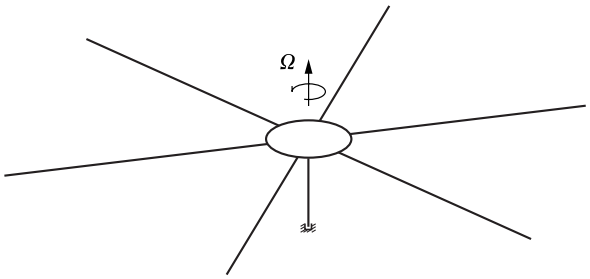

Figure 4. A rotary wing model with rigid hub.

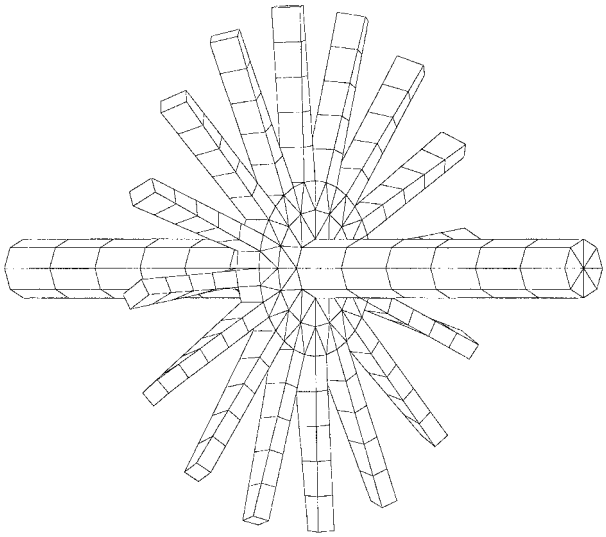

Figure 5. A simplified bladed disk–shaft turbine model.

A nomenclature list appears in the Appendix. The above equation can be written as a state differential equation

$$\begin{bmatrix} \mathbf{A}_{ii}^r & \mathbf{A}_{ij}^r \\ \mathbf{A}_{ji}^r & \mathbf{A}_{jj}^r \end{bmatrix} \begin{Bmatrix} \dot{\mathbf{y}}_i^r \\ \dot{\mathbf{y}}_j^r \end{Bmatrix} + \begin{bmatrix} \mathbf{B}_{ii}^r & \mathbf{B}_{ij}^r \\ \mathbf{B}_{ji}^r & \mathbf{B}_{jj}^r \end{bmatrix} \begin{Bmatrix} \mathbf{y}_i^r \\ \mathbf{y}_j^r \end{Bmatrix} = \begin{Bmatrix} \mathbf{F}_i^r \\ \mathbf{F}_j^r \end{Bmatrix} + \begin{Bmatrix} \mathbf{0} \\ \bar{\mathbf{F}}_j^r \end{Bmatrix}, \tag{2}$$

where the system matrices

$$\mathbf{A}_{kl}^r = \begin{bmatrix} (\mathbf{G}_{kl}^r + \mathbf{C}_{kl}^r) & \mathbf{M}_{kl}^r \\ -\mathbf{M}_{kl}^r & \mathbf{0} \end{bmatrix}, \quad \mathbf{B}_{kl}^r = \begin{bmatrix} \mathbf{K}_{kl}^r & \\ & \mathbf{M}_{kl}^r \end{bmatrix},$$

and state variables

$$\mathbf{y}_k^r = \begin{Bmatrix} \mathbf{x}_k^r \\ \dot{\mathbf{x}}_k^r \end{Bmatrix}, \quad \text{forces} \quad \mathbf{F}_k^r = \begin{Bmatrix} \mathbf{f}_k^r \\ \mathbf{0} \end{Bmatrix}, \quad \bar{\mathbf{F}}_k^r = \begin{Bmatrix} \bar{\mathbf{f}}_k^r \\ \mathbf{0} \end{Bmatrix}, \quad (k, l = i, j).$$

Introducing the following transformation between the state variables $\mathbf{y}_j^r$ and generalized co-ordinates $\mathbf{q}^r$, and a new set of generalized coordinates $\bar{\mathbf{y}}^r$, for the rth substructure

$$\begin{Bmatrix} \mathbf{y}_i^r \\ \mathbf{y}_j^r \end{Bmatrix} = \begin{bmatrix} \boldsymbol{\phi}_s^r & \boldsymbol{\phi}_c^r \\ \mathbf{0} & \mathbf{I} \end{bmatrix} \begin{Bmatrix} \mathbf{q}^r \\ \mathbf{y}_j^r \end{Bmatrix} = \boldsymbol{\Psi}^r \bar{\mathbf{y}}, \quad r = 1, \cdots, n+1, \tag{3}$$

where

$$\boldsymbol{\phi}_c^r = \begin{bmatrix} (\mathbf{K}_{ii}^r)^{-1} \mathbf{K}_{ij}^r & \\ & (\mathbf{K}_{ii}^r)^{-1} \mathbf{K}_{ij}^r \end{bmatrix}, \quad \boldsymbol{\Psi}^r = \begin{bmatrix} \boldsymbol{\phi}_s^r & \boldsymbol{\phi}_c^r \\ \mathbf{0} & \mathbf{I} \end{bmatrix}, \quad \bar{\mathbf{y}}^r = \begin{Bmatrix} \mathbf{q}^r \\ \mathbf{y}_j^r \end{Bmatrix}.$$

Modal matrix $\boldsymbol{\phi}_s^r$ can be obtained by the following substructure analysis:

Step 1: due to a fixed interface, $\mathbf{B}_{ii}^r$ is symmetric and positive definite. Applying a Cholesky decomposition for $\mathbf{B}_{ii}^r$, one has:

$$\mathbf{B}_{ii}^r = \mathbf{L}_B^r \mathbf{L}_B^{r\mathrm{T}}. \tag{4}$$

Step 2: find the eigensolution for matrix $(\mathbf{L}_B^r)^{-1}\mathbf{A}_{ii}^r(\mathbf{L}_B^r)^{-\mathrm{T}}$

$$(\mathbf{X}_{ii}^r)^{-1}[(\mathbf{L}_B^r)^{-1}\mathbf{A}_{ii}^r(\mathbf{L}_B^r)^{-\mathrm{T}}]\mathbf{X}_{ii}^r = \mathrm{block}-\mathrm{diag}\{\mathbf{J}_1^r, \mathbf{J}_2^r, \cdots, \mathbf{J}_{m_s^r}^r\} = \mathbf{\Lambda}^r, \tag{5}$$

where $\mathbf{\Lambda}^r$ is the Jordan form of matrix $(\mathbf{L}_B^r)^{-1}\mathbf{A}_{ii}^r(\mathbf{L}_B^r)^{-\mathrm{T}}$, with Jordan blocks

$$\mathbf{J}_k^r = \begin{bmatrix} \lambda_k^r & 1 & & \\ & \lambda_k^r & \ddots & \\ & & \ddots & 1 \\ & & & \lambda_k^r \end{bmatrix}, \quad (k = 1, \cdots, m_s^r) \tag{6}$$

arranged from lower to higher frequencies.

Step 3: defining $\mathbf{\phi}_s^r = (\mathbf{L}_B^r)^{-\mathrm{T}}\,\mathbf{X}_{ii}^r$ and $\bar{\mathbf{\phi}}_s^r = (\mathbf{X}_{ii}^r)^{-1}(\mathbf{L}_B^r)^{-1}$, one has

$$(\bar{\mathbf{\phi}}_s^r)^{\mathrm{T}}\mathbf{A}_{ii}^r\mathbf{\phi}_s^r = \mathbf{\Lambda}^r, \quad (\bar{\mathbf{\phi}}_s^r)^{\mathrm{T}}\mathbf{B}_{ii}^r\mathbf{\phi}_s^r = \mathbf{I}^r$$

and

$$\mathbf{A}_{ii}^r\mathbf{\phi}_s^r = \mathbf{B}\mathbf{\phi}_s^r\mathbf{\Lambda}^r. \tag{7a, b; 8}$$

Substituting equation (3) into equation (2), and premultiplying it by $(\bar{\mathbf{\psi}}^r)^{\mathrm{T}}$, it follows

$$\bar{\mathbf{A}}^r\dot{\bar{\mathbf{y}}} + \bar{\mathbf{B}}^r\bar{\mathbf{y}}^r = \bar{\mathbf{F}}^r + \tilde{\mathbf{F}}_j^r, \quad r = 1, \cdots, n+1, \tag{9}$$

where

$$\bar{\mathbf{A}}^r = (\bar{\mathbf{\psi}}^r)^{\mathrm{T}}\mathbf{A}^r\mathbf{\Psi}^r = \begin{bmatrix} \mathbf{\Lambda}^r & \bar{\mathbf{A}}_{ij}^r \\ \bar{\mathbf{A}}_{ji}^r & \bar{\mathbf{A}}_{jj}^r \end{bmatrix}, \quad \bar{\mathbf{B}}^r = (\bar{\mathbf{\Psi}}^r)^{\mathrm{T}}\mathbf{B}^r\mathbf{\Psi}^r = \begin{bmatrix} \mathbf{I}^r & \mathbf{B}_{ij}^r \\ \mathbf{B}_{ji}^r & \mathbf{B}_{jj}^r \end{bmatrix},$$

$$\bar{\mathbf{F}}^r = (\bar{\mathbf{\Psi}}^r)^{\mathrm{T}}\begin{Bmatrix} \mathbf{F}_i^r \\ \mathbf{F}_j^r \end{Bmatrix}, \quad \hat{\mathbf{F}}_j^r = (\bar{\mathbf{\Psi}}^r)^{\mathrm{T}}\begin{Bmatrix} \mathbf{0} \\ \bar{\mathbf{F}}_j^r \end{Bmatrix}, \quad \bar{\mathbf{\Psi}}^r = \begin{bmatrix} \bar{\mathbf{\phi}}_s^r & \mathbf{\phi}_c^r \\ \mathbf{0} & \mathbf{I} \end{bmatrix}.$$

3. SYNTHESIS BASED ON THE RIGID DISK

On each interface node, the transitional and rotational displacements must be compatible with the displacements of the rigid body, and all the forces and moments from the substructure interfaces to the rigid body and its inertial and damping forces are in equilibrium, therefore,

$$\mathbf{y}_j^r = (\mathbf{T}^r)^{\mathrm{T}}\mathbf{y}_h, \quad \mathbf{A}_h\dot{\mathbf{y}}_h + \mathbf{B}_h\mathbf{y}_h = -\sum_{r=1}^{n+1}\mathbf{T}^r\hat{\mathbf{F}}_j^r \quad r = 1, 2, \cdots, n+1 \tag{10a, b}$$

where equation (10b) is the linearized governing equation of motion in the state space for the hub rigid disk and

$$\mathbf{A}_h = \begin{bmatrix} (\mathbf{G}_h + \mathbf{C}_h) & \mathbf{M}_h \\ -\mathbf{M}_h & \mathbf{0} \end{bmatrix}, \quad \mathbf{B}_h = \begin{bmatrix} \mathbf{0} & \mathbf{0} \\ \mathbf{0} & \mathbf{M}_h \end{bmatrix}, \quad \mathbf{y}_h = \begin{Bmatrix} \mathbf{x}_h \\ \dot{\mathbf{x}}_h \end{Bmatrix},$$
$$\mathbf{T}^r = [\bar{\mathbf{T}}_1^r \quad \bar{\mathbf{T}}_2^r \quad \cdots \quad \bar{\mathbf{T}}_{n_k}^r] \qquad (r = 1, \cdots, n). \tag{11}$$

Considering equation (11), $\bar{\mathbf{T}}_i^r$ $(i = 1, \cdots, n_k)$ takes the following form

$$\bar{\mathbf{T}}_i^r = \begin{bmatrix} \hat{\mathbf{T}}_i^r & \\ & \hat{\mathbf{T}}_i^r \end{bmatrix}. \tag{12}$$

For $\hat{\mathbf{T}}_i^r$, let

$$\tilde{\mathbf{T}}_i^r = \begin{bmatrix} \cos\theta_i^r & -\sin\theta_i^r & 0 \\ \sin\theta_i^r & \cos\theta_i^r & 0 \\ 0 & 0 & 1 \end{bmatrix},$$
$$R_i^r = \begin{bmatrix} 0 & -z_i & (d_i/2)\sin\theta_i^r \\ z_i & 0 & -(d_i/2)\cos\theta_i^r \\ -(d_i/2)\sin\theta_i^r & (d_i/2)\cos\theta_i^r & 0 \end{bmatrix},$$

then,

$$\hat{\mathbf{T}}_i^r = \begin{bmatrix} \tilde{\mathbf{T}}_i^r & 0 \\ (\mathbf{R}_i^r\tilde{\mathbf{T}}_i^r) & \tilde{\mathbf{T}}_i^r \end{bmatrix},$$

or explicitly

$$\hat{\mathbf{T}}_i^r = \begin{bmatrix} \cos\theta_i^r & -\sin\theta_i^r & 0 & 0 & 0 & 0 \\ \sin\theta_i^r & \cos\theta_i^r & 0 & 0 & 0 & 0 \\ 0 & 0 & 1 & 0 & 0 & 0 \\ -z_i\sin\theta_i^r & -z_i\cos\theta_i^r & (d_i/2)\sin\theta_i^r & \cos\theta_i^r & -\sin\theta_i^r & 0 \\ z_i\cos\theta_i^r & -z_i\sin\theta_i^r & -(d_i/2)\cos\theta_i^r & \sin\theta_i^r & \cos\theta_i^r & 0 \\ 0 & 1 & 0 & 0 & 0 & 1 \end{bmatrix}. \tag{13}$$

The transformation of the ith nodal co-ordinate on the interface of the rth substructure to the global co-ordinate is illustrated in Figure 6.

The assembled equations for the whole structure can be obtained by combining equations (9), (10a) and (10b) as

$$\tilde{\mathbf{A}}\dot{\tilde{\mathbf{y}}} + \tilde{\mathbf{B}}\tilde{\mathbf{y}} = \tilde{\mathbf{F}}, \tag{14}$$

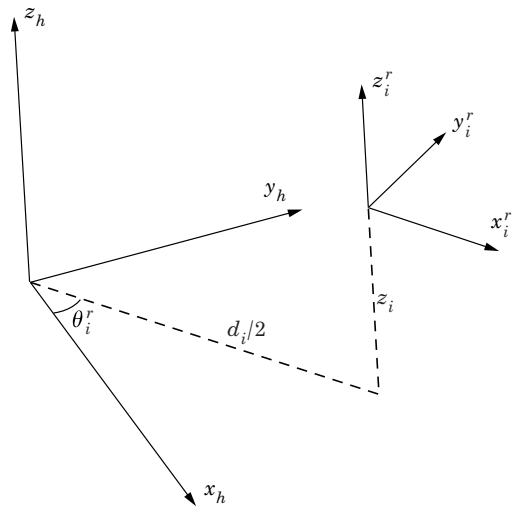

Figure 6. Local and global co-ordinate systems.

where

$$\tilde{\mathbf{A}} = \begin{bmatrix} \boldsymbol{\Lambda}^1 & & & & \bar{\mathbf{A}}_{ij}^1(\mathbf{T}^1)^{\mathrm{T}} \\ & \ddots & & & \vdots \\ & & \boldsymbol{\Lambda}^n & & \bar{\mathbf{A}}_{ij}^n(\mathbf{T}^r)^{\mathrm{T}} \\ & & & \boldsymbol{\Lambda}^{n+1} & \bar{\mathbf{A}}_{ij}^{n+1}(\mathbf{T}^{n+1})^{\mathrm{T}} \\ \mathbf{T}^1\bar{\mathbf{A}}_{ji}^1 & \cdots & \mathbf{T}^n\bar{\mathbf{A}}_{ji}^1 & \mathbf{T}^{n+1}\bar{\mathbf{A}}_{ji}^1 & \left(\sum_{r=1}^{n+1}\mathbf{T}^r\bar{\mathbf{A}}_{jj}^r\mathbf{T}^{r^{\mathrm{T}}} + \mathbf{A}_h\right) \end{bmatrix},$$

$$\tilde{\mathbf{B}} = \begin{bmatrix} \mathbf{I}^1 & & & & \bar{\mathbf{B}}_{ij}^1(\mathbf{T}^1)^{\mathrm{T}} \\ & \ddots & & & \vdots \\ & & \mathbf{I}^n & & \bar{\mathbf{B}}_{ij}^n(\mathbf{T}^n)^{\mathrm{T}} \\ & & & \mathbf{I}^{n+1} & \bar{\mathbf{B}}_{ij}^{n+1}(\mathbf{T}^{n+1})^{\mathrm{T}} \\ \mathbf{T}^1\bar{\mathbf{B}}_{ji}^1 & \cdots & \mathbf{T}^n\bar{\mathbf{B}}_{ji}^n & \mathbf{T}^{n+1}\bar{\mathbf{B}}_{ji}^{n+1} & \left(\sum_{r=1}^{n+1}\mathbf{T}^r\bar{\mathbf{B}}_{jj}^r(\mathbf{T}^r)^{\mathrm{T}} + \mathbf{B}_h\right) \end{bmatrix},$$

$$\tilde{\mathbf{y}} = \begin{Bmatrix} q^1 \\ \vdots \\ q^{n+1} \\ y_h \end{Bmatrix}.$$

Matrices $\tilde{\mathbf{A}}$ and $\tilde{\mathbf{B}}$ possess a nature of the block structure at the same level as substructures because the block feature reflects the geometric characteristics of the original structure.

4. VIBRATION CHARACTERISTICS

With the block structure of the assembled system matrices obtained by the dynamic substructure method, the qualitative properties of the whole structure can now be discussed.

Proposition: *For a structure containing n repetitive substructures mounted on a rigid body, which are oriented by rotation about a fixed axis in space, and connected to the rest of the structure only through the rigid body, (1) each eigenvalue of the repetitive substructure with a fixed interface is one of the at least $(n-3)$-multiple eigenvalues of the whole structure; (2) corresponding to each mode of the repetitive substructure with the fixed interface, the whole structure has $(n-3)$ independent mode shapes, which are combinations of the modes from the repetitive substructures.*

Proof: the eigenvalue problem defined by equation (14) can be written as:

$$(\tilde{\mathbf{A}} + \mu\tilde{\mathbf{B}})\tilde{\mathbf{y}} = 0. \tag{15a}$$

Adopting full principal modes in the transformation (3), the characteristic equation (15a) becomes equivalent to the eigenvalue problem for the whole structure. If for a test number μ, the number of independent solutions $\tilde{\mathbf{y}}$ to equation (15a) is α, μ will be at least $(2N-\alpha)$ multiple eigenvalues of the system. First, trying a μ with a non-defective eigenvalue λ_k of the repetitive substructures with a fixed interface, equation (15a) will be in the following form:

$$\begin{pmatrix} (\lambda_k\mathbf{I}^1 + \mathbf{\Lambda}^1) & & & & (\bar{\mathbf{A}}_{ij}^1 + \lambda_k\bar{\mathbf{B}}_{ij}^1)\mathbf{T}^{1\mathrm{T}} \\ & \ddots & & & \vdots \\ & & (\lambda_k\mathbf{I}^n + \mathbf{\Lambda}^n) & & (\bar{\mathbf{A}}_{ij}^n + \lambda_k\bar{\mathbf{B}}_{ij}^n)\mathbf{T}^{n\mathrm{T}} \\ & & & (\lambda_k\mathbf{I}^{n+1} + \mathbf{\Lambda}^{n+1}) & (\bar{\mathbf{A}}_{ij}^n + \lambda_k\bar{\mathbf{B}}_{ij}^n)(\mathbf{T}^{n+1})^{\mathrm{T}} \\ \mathbf{T}^1(\bar{\mathbf{A}}_{ji}^1 + \lambda_k\bar{\mathbf{B}}_{ji}^1) & \cdots & \mathbf{T}^n(\bar{\mathbf{A}}_{ji}^n + \lambda_k\bar{\mathbf{B}}_{ji}^n) & \mathbf{T}^{n+1}(\bar{\mathbf{A}}_{ji}^{n+1} + \lambda_k\bar{\mathbf{B}}_{ji}^{n+1}) & \sum_{r=1}^{n+1}\mathbf{T}^r(\bar{\mathbf{A}}_{jj}^r + \lambda_k\bar{\mathbf{B}}_{jj}^r) \\ & & & & \cdot(\mathbf{T}^r)^{\mathrm{T}} \end{pmatrix}$$

$$\cdot\bar{\mathbf{y}} = \mathbf{0} \tag{15b}$$

Denoting $\mathbf{q}^r$ for the mode of the repetitive substructure corresponding to λ_k, taking

$$\tilde{\mathbf{y}} = \begin{Bmatrix} \alpha^1 \tilde{q} \\ \vdots \\ \alpha^n \tilde{q} \\ 0 \\ 0 \end{Bmatrix}, \tag{16}$$

and substituting the above vector into equation (15b), according to the definition of $\tilde{\mathbf{y}}$, one obtains automatically the first $(n+1)$ block equations of (15b). The last block equation of equation (15b) will be satisfied if

$$\sum_{r=1}^{n} \alpha^r \mathbf{T}^r = 0. \tag{17}$$

From equations (11), (12) and (13), there are only $2 \times n_k + 1$ independent equations in the matrix equation (17), i.e.,

$$\begin{cases} \alpha^1 + \alpha^2 + \cdots + \alpha^n = 0 \\ \alpha^1 \cos\theta_1^1 + \alpha^2 \cos\theta_1^2 + \cdots + \alpha^n \cos\theta_1^n = 0 \\ \alpha^1 \sin\theta_1^1 + \alpha^2 \sin\theta_1^2 + \cdots + \alpha^n \sin\theta_1^n = 0 \\ \quad \cdot \qquad\quad \cdot \qquad\quad \cdot \\ \alpha^1 \cos\theta_{n_k}^1 + \alpha^2 \cos\theta_{n_k}^2 + \cdots + \alpha^n \cos\theta_{n_k}^n = 0 \\ \alpha^1 \sin\theta_{n_k}^1 + \alpha^2 \sin\theta_{n_k}^2 + \cdots + \alpha^n \sin\theta_{n_k}^n = 0 \end{cases}. \tag{18}$$

From the assumption that all blade substructures are oriented by rotation about a fixed axis in space, the azimuthal angles of the node on the interface between the blade substructure and the rigid disk satisfy the following relationships, i.e.,

$$(\theta_1^{r+1} - \theta_1^r) = \cdots = (\theta_i^{r+1} - \theta_i^r) = \cdots = (\theta_{n_k}^{r+1} - \theta_{n_k}^r), \quad (r = 1, \cdots, n-1). \tag{19}$$

Taking equation (19) into consideration, the number of independent equations in equation (18) can be reduced to 3 by direct trigonometric manipulations, which can be written in matrix form as

$$\begin{bmatrix} \cos\theta_i^1 & \cos\theta_i^2 & \cdots & \cos\theta_i^n \\ \sin\theta_i^1 & \sin\theta_i^2 & \cdots & \sin\theta_i^n \\ 1 & 1 & \cdots & 1 \end{bmatrix} \begin{Bmatrix} \alpha^1 \\ \vdots \\ \alpha^n \end{Bmatrix} = 0, \tag{20}$$

where i may be an arbitrary number belonging to $\{1, \cdots, n_k\}$. According to the matrix theory, the number of independent non-trivial solutions for equation (20) is at least $(n-3)$.

Supposing that the repetitive substructure has a defective eigenvalue λ_k, its Jordan block and the associated principal mode matrix are assumed to be $\mathbf{J}_k$ and $\mathbf{Q}_J$, respectively; then

$$\tilde{\mathbf{A}}\tilde{\mathbf{Y}}_{\mathbf{J}} = \mathbf{B}\tilde{\mathbf{Y}}_{\mathbf{J}}\mathbf{J}_{\mathbf{k}}, \tag{21}$$

where

$$\tilde{\mathbf{Y}}_J = \begin{Bmatrix} \alpha^1 Q_J \\ \vdots \\ \alpha^n Q_J \\ 0 \\ 0 \end{Bmatrix}. \tag{22}$$

The number of solutions $\{\alpha^1, \cdots, \alpha^n\}$ which satisfy equation (21), is also $(n-3)$.

From the physics point of view, if for a mode of the whole structure, the interface forces and moments from repetitive substructures are in equilibrium for the rigid body, the mode behaves as if the rest of the structure is rigid. In such a case, the frequencies of the single repetitive substructure appear as the frequencies of the whole structure. The proposition shows that the multiple eigenvalues arising from the repetition of the substructures introduce no new defectiveness to the eigenvalue problem of the whole structure.

5. NUMERICAL EXAMPLES

5.1. EXAMPLE 1. ROTARY WING MODELS WITH A RIGID HUB

From the theoretical results in the previous section, each eigenvalue of the single blade with root fixed is at least 1, 3, 6 multiple eigenvalues, respectively, of the 4, 6, 9 bladed rotary wing model with a rigid hub. The numerical results on a gyroscopic eigenvalue problem for the single blade, the 4, 6, 9-bladed rotary wing models, are listed in Tables 1–4, respectively. The blade parameters are: $E = 2{\cdot}1 \times 10^{11}$ pa, $\nu = 0{\cdot}3$, $\rho_l = 1{\cdot}13 \times 10^{-1}$ kg/m, cross-section $J_y = 1{\cdot}167 \times 10^{-11}$ m^4, $J_z = 1{\cdot}167 \times 10^{-8}$ m^4, $A = 2{\cdot}231 \times 10^{-5}$ m^2, blade length $l_b = 0{\cdot}508$ m. The shaft parameters are: $E = 2{\cdot}1 \times 10^{12}$ pa, $\nu = 0{\cdot}3$, $\rho_l = 1{\cdot}13 \times 10^{-1}$ kg/m, $J_y = J_z = 1{\cdot}167 \times 10^{-8}$ m^4, $A = 2{\cdot}231 \times 10^{-5}$ m^2, shaft length $l_s = 0{\cdot}2$ m. The diameter of the rigid disk: $d = 0{\cdot}2032$ m, the mass, inertial moments about the rotation axis and diameter: $m_d = 1$ kg, $I_R = 0{\cdot}2$ kg m^4, $I_d = 0{\cdot}1$ kg m^4. The rotating speed of the model: $\Omega = 300$ r.p.m. The method for solving eigenvalue problems described in references [9, 12] was adopted.

5.2. EXAMPLE 2. A SIMPLIFIED TURBINE MODEL

As shown in Figure 5, this model has 16 turbine blades. For simplicity, the non-rotating eigenvalue problem is solved with brick elements in the finite element modelling. The frequencies of the single blade with its root fixed are shown in Table 5. The rigid hub disk was simulated by brick elements with a high elastic modulus. From Tables 6a–c, one can see the convergence of the

TABLE 1

The first four frequencies of the blade (rad/s)

72·0667	**413·175**	**1132·14**	**1994·81**

TABLE 2

The first 18 *frequencies of the* 4*-bladed rotary wing model* (rad/s)

71·9539	71·9541	72·0665	**72·0667**	207·084	328·362
329·768	413·169	**413·175**	414·242	414·263	1132·10
1132·14	1132·29	1132·29	1706·79	1723·35	**1994·81**

TABLE 3

The first 27 *frequencies of the* 6*-bladed rotary wing model* (rad/s)

71·8975	71·8980	72·0664	**72·0667**	**72·0667**	**72·0667**	
202·588	326·038	328·104	413·166	**413·175**	**413·175**	**413·175**
414·714	414·759	1132·08	**1132·14**	**1132·14**	**1132·14**	1132·36
1132·26	1637·26	16597·07	**1994·81**	**1994·81**	**1994·81**	2134·84

TABLE 4

The first 40 *frequencies of the* 9*-bladed rotary wing model* (rad/s)

71·8131	71·8142	72·0663	**72·0667**	**72·0667**	**72·0667**	**72·0667**
72·0667	**72·0667**	196·377	322·654	325·685	413·161	**413·175**
413·175	**413·175**	**413·175**	**413·175**	**413·175**	415·358	415·449
1132·04	**1132·14**	**1132·14**	**1132·14**	**1132·14**	**1132·14**	**1132·14**
1132·44	1132·45	1554·38	1577·71	**1994·81**	**1994·81**	
1994·81	**1994·81**	**1994·81**	**1994·81**	2200·92	2221·36	

TABLE 5

The first four frequencies of the turbine blade (rad/s)

833·861	1375·13	4294·32	4933·46

TABLE 6

The first 18 frequencies of the 16-bladed turbine model (rad/s)

(a) Disk elastic modulus: $E = 2{\cdot}1 \times 10^{11}$ pa

290·05	544·66	544·67	807·90	808·02	808·02	808·38	808·39	808·97
808·97	809·60	809·95	810·73	810·73	811·47	811·47	813·65	813·65

(b) Disk elastic modulus: $E = 2{\cdot}1 \times 10^{13}$ pa

292·47	561·54	651·54	833·57	833·57	833·58	833·58	833·58	833·59
833·59	833·59	833·60	833·60	833·60	833·61	833·61	933·52	933·53

(c) Disk elastic modulus: $E = 2{\cdot}1 \times 10^{15}$ pa

292·49	561·76	561·76	**833·85**	**833·85**	**833·85**	**833·86**	**833·86**	**833·86**
833·86	**833·86**	**833·86**	**833·86**	**833·86**	**833·86**	**833·87**	934·37	934·37

multiple eigenvalues to that of the single blade as the elastic modulus of the disk increases from $2{\cdot}1 \times 10^{11}$ pa to $2{\cdot}1 \times 10^{13}$ pa and to $2{\cdot}1 \times 10^{15}$ pa. The diameters of the shaft and the disk are 0·2 m and 0·6 m, respectively. The end-to-end length of the shaft is 2·5 m. The thickness of the disk is 0·1 m. The blades all have uniform cross-section: 0·1 m $\times$ 0·59 m with a length 0·6 m. All blades have a uniform pre-twist of 50°/m, but still being oriented in the direction of the disk radius. The material properties of the blade and the shaft are $E = 2{\cdot}1 \times 10^{11}$ pa, $\nu = 0{\cdot}3$, $\rho = 7800$ kg/m^3. The mass density of the disk is also 7800 kg/m^3.

6. CONCLUSION

The procedure of obtaining analytical results in this paper has demonstrated that the dynamic substructure method has the potential to be used to investigate the dynamic characteristics qualitatively for those structures containing repetitive components because the symmetry of a structure can be retained in the analytical expressions. The results of multiple eigenvalues of the bladed disk–shaft system and their non-defectiveness have enriched the understanding to the dynamic characteristics of that type of structures. One may anticipate that the multiple eigenvalues arising from other types of geometric repetition or symmetry do not introduce defectiveness to the structural systems, either.

ACKNOWLEDGMENTS

This research was funded and supported by the National Science Foundation of China: No. 19672033 and National Key Project on Basic Research and Applied Research: "The Research of Some Key Techniques of Dynamics of Large-Scale Mechanical and Electrical systems".

REFERENCES

1. J. H. WILKINSON 1965 *The Algebraic Eigenvalue Problem*. Oxford: Clarendon Press.
2. C. C. PAIGE 1970 *Ph.D. Thesis, University of London*. The computation of eigenvalues and eigenvectors of very large sparse matrices.
3. G. H. GOLUB and C. F. VAN LOAN 1989 *Matrix Computations*. Baltimore and London: The John Hopkins University Press.
4. R. R. CRAIG 1981 *Structural Dynamics*. New York: John Wiley.
5. L. MEIROVITCH 1980 *Computational Methods in Structural Dynamics*. Alphen aan den Rijn, The Netherlands: Sijthoff and Noordhoff.
6. D. J. EWINS 1984 *Modal Testing: Theory and Practice*. New York: John Wiley.
7. R. GREIF 1986 *Shock and Vibration Digest* **18**(7), 3–8. Substructuring and component mode synthesis.
8. Z. C. ZHENG, X. P. ZHOU and D. B. LI 1985 *ASME* 85-*IGT*-73, 1–7. Gyroscopic mode synthesis in the dynamic analysis of a multishaft rotor-bearing system.
9. G. X. REN 1993 *Ph.D. Thesis, Tsinghua University*. Numerical methods for large scale gyroscopic eigenvalue problems.
10. Z. C. ZHENG and G. X. REN 1994 *Proceedings of the Fourth International Conference on Rotor Dynamics*, Chicago, 255–260. Eigensolution of the rotary wing system.

11. G. X. REN, Z. C. ZHENG and J. G. CHENG 1997 *American Institute of Aeronautics and Astronautics Journal* **35**, 355–361. Multiple eigenvalues arising from a class of repetitive substructures.
12. Z. C. ZHENG, G. X. REN and W. J. WANG 1996 *Journal of Sound and Vibration* **199**, 253–268. A reduction method for unsymmetrical eigenvalue problem in structural dynamics.

APPENDIX: NOMENCLATURE

$(\cdot)^r$ variable $(\cdot)$ is related to the rth substructure
$\mathbf{M}^r$ mass matrix of the rth substructure, positive definite
$\mathbf{G}^r$ gyroscopic matrix of the rth substructure, skew symmetric
$\mathbf{C}^r$ damping matrix of the rth substructure, symmetric
$\mathbf{K}^r$ stiffness matrix of the rth substructure, semi-positive definite
$\mathbf{x}^r$ the nodal displacement vector for the rth substructure
$\mathbf{f}^r$ external force vector exerted on the rth substructure
$\bar{\mathbf{f}}^r$ internal force vector exerted on the interface of the rth substructure
$\mathbf{M}_h$ the linearized mass matrix of the hub rigid disk, size 6×6
$\mathbf{G}_h$ the gyroscopic matrix of the hub rigid disk, size 6×6
$\mathbf{C}_h$ the damping matrix of the hub rigid disk, size 6×6
i index of internal variables for substructures
j index of interface variables for substructures
N number of degrees of freedom of the whole structure with the FEM discretization
m_i^r number of degrees of freedom of the internal part of the rth substructure
m_j^r number of degrees of freedom of the interface part of the rth substructure
m_s^r number of retained Jordan blocks for the rth substructure
q generalized co-ordinate
$\bar{\boldsymbol{\phi}}_s^r$ the left principal mode matrix of the rth substructure with interface fixed, size $2m_i^r \times m_s^r$
$\boldsymbol{\phi}_s^r$ the right principal mode matrix of the rth substructure with interface fixed, size $2m_i^r \times m_s^r$
$\boldsymbol{\phi}_c^r$ the constraint mode matrix of the rth substructure, $2m_i^r \times 2m_j^r$
$\mathbf{T}_r$ the transformation between the interface co-ordinates in the local co-ordinate system of the rth substructure and the global co-ordinate system
$\mathbf{x}$ displacement vector
$\mathbf{x}_h$ the linearized displacement vector of the hub rigid body, including 3 translation and 3 rotation displacements, size 6×1
$\mathbf{y}_h$ the state vector of the hub rigid body in global co-ordinate system, size 12×1
n_k the number of nodes on the interface between the blades and the rigid hub disk
θ_i^r the azimuthal angle of the ith node in the interface of the rth blade and the disk
z_i the axial co-ordinate of the ith node in all the interfaces between blades and the disk

d_i the diameter of the circle on which the ith node on interfaces between blades and the disk are positioned